

# Supplementary material for “Strong reconnection electric fields in shock-driven turbulence”

Fig. S1 shows the electron-only reconnection region corresponding to Fig. 2. Plot (a) shows the electron in-plane velocity  $V_e = (V_{ex}^2 + V_{ey}^2)^{1/2}$  in the X-line rest frame. The orange oval regions represent the three inflow regions, and the red oval region is the outflow region. The  $L$  axis is the same as the  $L$  axis in Fig. 2(d), and the  $L'$  axis is parallel to the  $y$  axis, along the outflow. The  $N'$  axis is parallel to the  $N$  axis in Fig. 2(d), but slightly shifted to the positive  $x$  direction with  $0.15d_i$ , so that we can plot the inflow profile in the two orange oval regions along this axis. Panel (b) shows the 1D profile of  $V_{eL'}$  along  $L'$ , which is the outflow in the red oval region, and the profile of  $V_{eL}$  along  $L$ , which is the inflow in the orange oval region along  $L$ . There is an  $L$ -directional inflow in  $y_X < y$  that has a negative  $V_{eL}$ , and it is connected to the outflow. The outflow  $V_{eL'}$  shows a negative peak  $\sim -10v_{A0}$  at  $y = 25.8d_i$ . Panel (c) shows the 1D profile of the inflow along  $N'$ . There are converging inflows toward the magnetic neutral line. Panel (d) shows the non-ideal electric field  $E'_{z-e} = E_z + (\mathbf{V}_e \times \mathbf{B})_z/c$  in the X-line rest frame, and the region surrounded by red lines is the EDR. We decided the EDR based on: (1) inside the EDR, electrons are unmagnetized, i.e.,  $|E'_{z-e}|$  is large, (2) bounded by the maxima of  $|B_L|$  in the inflow ( $N$ ) direction, (3) bounded by the outflow regions, which generate regions (outer EDR) that show  $E'_{z-e}$  whose sign is opposite to the region around the X-line (inner EDR). Near the X-line,  $E'_{z-e}$  becomes large positive (red color), which indicates electrons are strongly unmagnetized. The black dots represent the two maxima of  $|B_L|$  along the inflow ( $N$ ) direction (see Fig. 2(f)), and we chose these two points for the  $N$  boundaries of the EDR. The outflow region (left to the X-line) shows large negative  $E'_{z-e}$  (blue color), because the convection term  $(\mathbf{V}_e \times \mathbf{B})_z$  becomes dominant in  $E'_{z-e}$ , which is consistent with the two-scale EDR structure discussed by Shay et al. 2007 (PRL 99, 155002) for the standard reconnection, where the inner EDR and the outer EDR show opposite signs

of  $E'_{z-e}$ . Therefore, we chose the boundary of the negative  $E'_{z-e}$  region as the outflow side of the EDR boundary. For the positive- $L$  side, where an  $L$ -directional inflow exits, we chose the boundary near the end of positive  $E'_{z-e}$  region and where the  $L$ -directional inflow starts. Panel (e) shows the energy exchange rate  $\mathbf{J} \cdot \mathbf{E}'$ , where  $\mathbf{E}' = \mathbf{E} + \mathbf{V}_e \times \mathbf{B}/c$ . The EDR well corresponds to the region where  $\mathbf{J} \cdot \mathbf{E}'$  becomes large, which is consistent with the result by Zenitani et al. 2011 (PRL 106, 195003) for the standard reconnection.

Fig. S2 shows the electron-only reconnection region corresponding to Fig. 3. Plot (a) shows the electron in-plane velocity  $V_e$  in the X-line rest frame. The orange oval regions represent the inflow regions, and the red oval region is the outflow region. The  $L''$  axis is along the outflow in the lower left separatrix, and the  $L'$  axis is along the upper right separatrix region. The  $N'$  axis is parallel to the  $y$  axis, and this axis passes through the two inflow regions. Panel (b) shows the 1D profile of  $V_{eL''}$  along  $L''$  in  $y < y_X$ , which is the outflow in the red oval region, and the profile of  $V_{eL'}$  along  $L'$  in  $y_X < y$ . The outflow ( $V_{eL''}$  in  $y < y_X$ ) shows a negative value near  $-4v_{A0}$ , while there is a positive  $V_{eL'}$  flow in the region  $y_X < y$ . This positive  $V_{eL'}$  flow is part of the background flow, which is seen as an upward flow (red color in panel (a)) in the region right to the X-line. Panel (c) shows the 1D profile of the inflow along  $N'$ . There are converging inflows toward the X-line. Panel (d) shows the non-ideal electric field  $E'_{z-e} = E_z + (\mathbf{V}_e \times \mathbf{B})_z/c$  in the X-line rest frame, and the region surrounded by red lines is the EDR. The black dots represent the two maxima of  $|B_L|$  along the inflow ( $N$ ) direction (see Fig. 3(f)). The outflow region near  $x = 48.2d_i$  and  $y = 37.0d_i$  shows negative  $E'_{z-e}$  (blue color), which is a signature of the outer EDR, where the  $(\mathbf{V}_e \times \mathbf{B})$  term becomes dominant in  $E'_{z-e}$ . Panel (e) shows  $\mathbf{J} \cdot \mathbf{E}'$ . As explained in the text for Fig. 3, the X-line shows positive  $E_z$ , but the current density  $J_z$  is negative, and  $\mathbf{J} \cdot \mathbf{E}'$  at the X-line is negative. However, the surrounding regions show positive values, including the region of the strong outflow jet.

Fig. S3 shows the regular reconnection region corresponding to Fig. 7. Plot (a) shows the electron in-plane velocity  $V_e$  in the X-line rest frame. The orange oval regions represent the inflow regions, and the red oval regions are the outflow regions. The  $L'$  axis is along the outflows. The  $N$  axis is the same as the  $N$  axis shown in Fig. 7(d). Panel (b) shows the 1D profile of  $V_{eL'}$  along  $L'$ , the outflows in the red oval regions. The outflows form as bipolar two-sided jets, with the minimum  $\sim -8v_{A0}$  and the maximum  $\sim 12v_{A0}$ . Panel (c) shows the 1D profile of the inflow along  $N$ . There are converging

inflows toward the X-line, although the flow in  $x_X < x$  is noisy. Panel (d) shows the non-ideal electric field  $E'_{z-e} = E_z + (\mathbf{V}_e \times \mathbf{B})_z/c$  in the X-line rest frame, and the region surrounded by red lines is the EDR. The black dots represent the two maxima of  $|B_L|$  along the inflow ( $N$ ) direction (see Fig. 7(f)). The sign of  $E_z$  at the X-line is negative, and  $E'_{z-e}$  around the X-line is also negative. In contrast,  $E'_{z-e}$  in the outer EDR, where there are strong outflows, becomes mostly positive, although  $E'_{z-e}$  in the outer EDR is noisy. Panel (e) shows  $\mathbf{J} \cdot \mathbf{E}'$ . Near the X-line,  $\mathbf{J} \cdot \mathbf{E}'$  shows large positive values. Compared with  $\mathbf{J} \cdot \mathbf{E}'$  in the electron-only reconnection site in Fig. S1,  $\mathbf{J} \cdot \mathbf{E}'$  in this regular reconnection site is quite noisy, and the region of positive value spreads outside the EDR, even in the inflow region (the orange oval region in panel (a)) right to the X-line.

Fig. S4 shows the same regular reconnection region as Fig. S3, and plot (a) shows the ion in-plane velocity  $V_i$  in the X-line rest frame. The orange oval regions represent the inflow regions, and the red oval region is the outflow region. The outflow shows two peaks in the red oval region, indicated by the black dots; therefore, we use two axes, the  $L''$  and  $L'''$  axes, each of which passes through the X-line and each peak outflow position. The  $L'$  axis is parallel to the  $y$  axis, passing through the inflow region (lower orange oval). Panel (b) shows the 1D profile of  $V_{iL'}$  (inflow) along  $L'$  in  $y < y_X$ , and the two outflows in  $y_X < y$ :  $V_{iL''}$  along  $L''$  (red) and  $V_{iL'''}$  along  $L'''$  (black). The  $L'$ -directional inflow in  $y < y_X$  shows its maximum around  $7v_{A0}$ , but it reduces to  $5v_{A0}$  at the X-line. From the X-line, the ion flow is accelerated again, and the outflows in both the  $L''$  and  $L'''$  directions show peaks around  $7v_{A0}$ . Panel (c) shows the 1D profile of the inflow along  $N$ . There are converging inflows toward the X-line. Panel (d) shows the electric field  $E'_{z-i} = E_z + (\mathbf{V}_i \times \mathbf{B})_z/c$  in the X-line rest frame, and the region surrounded by red lines is the EDR. A large negative  $E'_{z-i}$  (dark blue) region is spread throughout the EDR, where ions are strongly unmagnetized, and the unmagnetization region is extended outside the EDR, too. Positive  $E'_{z-i}$  (green) regions located left and right to the X-line are also where ions are unmagnetized, as we see later.

Panel (e) compares the electron unmagnetization and the ion unmagnetization, using  $E'_{z-e}$  and  $E'_{z-i}$  normalized by the reconnection electric field  $E_r$  at the X-line. To reduce noise (especially in  $E'_{z-e}$ , see Fig. S3(d)), we smoothed  $E'_{z-j}$  ( $j = e$  or  $i$ ) using a smoothing window  $0.25d_i \times 0.25d_i$  around each grid point. The value  $|E'_{z-j}/E_r|$  represents the degree of unmagnetization. The vicinity of the X-line shows  $|E'_{z-j}/E_r|$  close to unity, where particles are strongly unmagnetized, while  $|E'_{z-j}/E_r| \ll 1$

indicates that particles are magnetized. The region surrounded by white lines is the EDR. The red region is where  $|E'_{z-j}/E_r| > 0.15$ . The upper panel of (e) shows that the red regions ( $|E'_{z-e}/E_r| > 0.15$ ) are mostly consistent with the regions with large  $|E'_{z-e}|$  in plot (d) in Fig. S3 (dark blue and red regions), and roughly concentrated near the EDR, even though some red regions are spread outside the EDR. Electrons are mostly unmagnetized in the EDR, and electrons outside the EDR are magnetized (green regions). Using the same threshold value ( $0.15E_r$ ) for the ions, the lower plot of (d) shows that ions are unmagnetized in almost the entire region. If the reconnection region were much larger as in the standard laminar reconnection, a clear boundary of the IDR would be seen. However, due to the small reconnection region in the shock turbulence, almost the entire reconnection region shows the signature of the ion unmagnetization. In contrast, the electron-unmagnetization regions are more localized near the reconnection region. Since ions are unmagnetized throughout the region, while electrons are unmagnetized in the EDR and magnetized away from the EDR, the diffusion region is almost like the EDR, and the ion unmagnetization does not play a major role to form the diffusion region, even though unmagnetized ions are accelerated due to the reconnection electric field.

Fig. S5 shows the in-plane electric fields  $E_x$  and  $E_y$  in the X-line rest frame in each reconnection region. Panels (a) and (b) are for the electron-only reconnection region corresponding to Fig. 2. Along the current sheet, there is a unipolar in-plane electric field with negative  $E_x$  and positive  $E_y$  (see the red oval region). This electric field resembles the Hall electric field in the standard asymmetric reconnection pointing toward the magnetic neutral line. Panels (c) and (d) show the electric fields in the electron-only reconnection region corresponding to Fig. 3. In this reconnection region, as Fig. 3 shows, there is a current sheet in the vertical direction, and the in-plane electric field forms also along the current sheet, pointing mainly in the negative  $x$  direction. Panels (e) and (f) are the regular reconnection region corresponding to Fig. 7. There is an almost unipolar  $E_x$  pointing to the negative  $x$  direction, which is the Hall electric field in asymmetric reconnection.

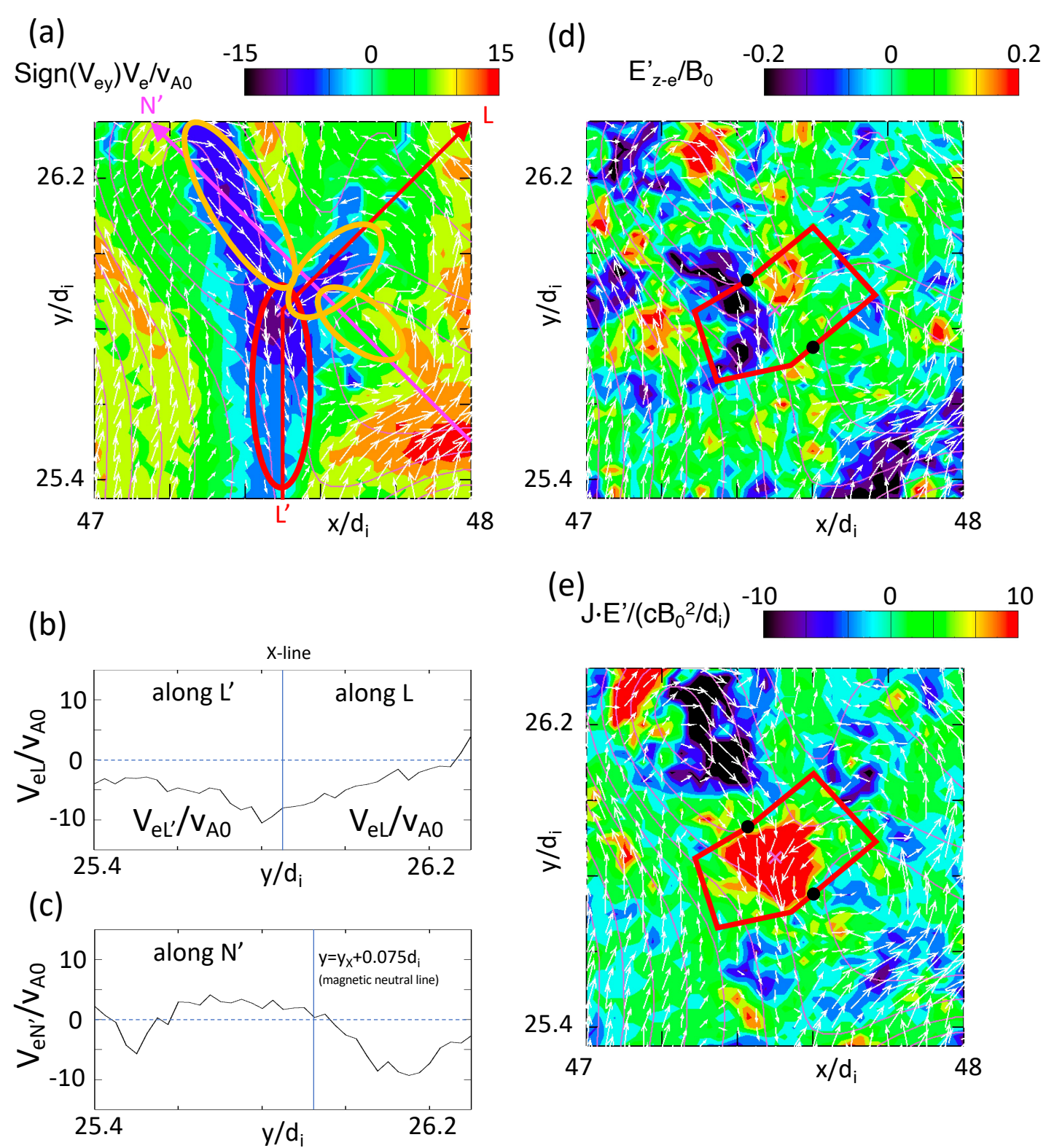


Fig. S1 Electron-only reconnection corresponding to Fig. 2. (a) Electron in-plane velocity  $V_e$  in the X-line rest frame. The orange and red ovals represent the inflow and outflow regions, respectively. The  $L$  axis is the same as in Fig. 2(d), and the  $L'$  axis is along the outflow. The  $N'$  axis is parallel to the  $N$  axis in Fig. 2(d), but shifted to the positive  $x$  direction (with  $0.15d_i$ ). The white arrows show the electron fluid velocity vectors. (b) The outflow profile along  $L'$ , and the inflow profile along  $L$ . The blue vertical line is the position of the X-line. (c) The inflow profile along  $N'$ . The blue vertical line is the position of the magnetic neutral line. (d) Contour of the electric field  $E'_{z-e} = E_z + (\mathbf{V}_e \times \mathbf{B})_z/c$ . The region surrounded by red lines represents the EDR. The black dots are the positions of the  $|B_z|$  maxima along the  $N$  axis. (e) Contour of  $\mathbf{J} \cdot \mathbf{E}'$ .

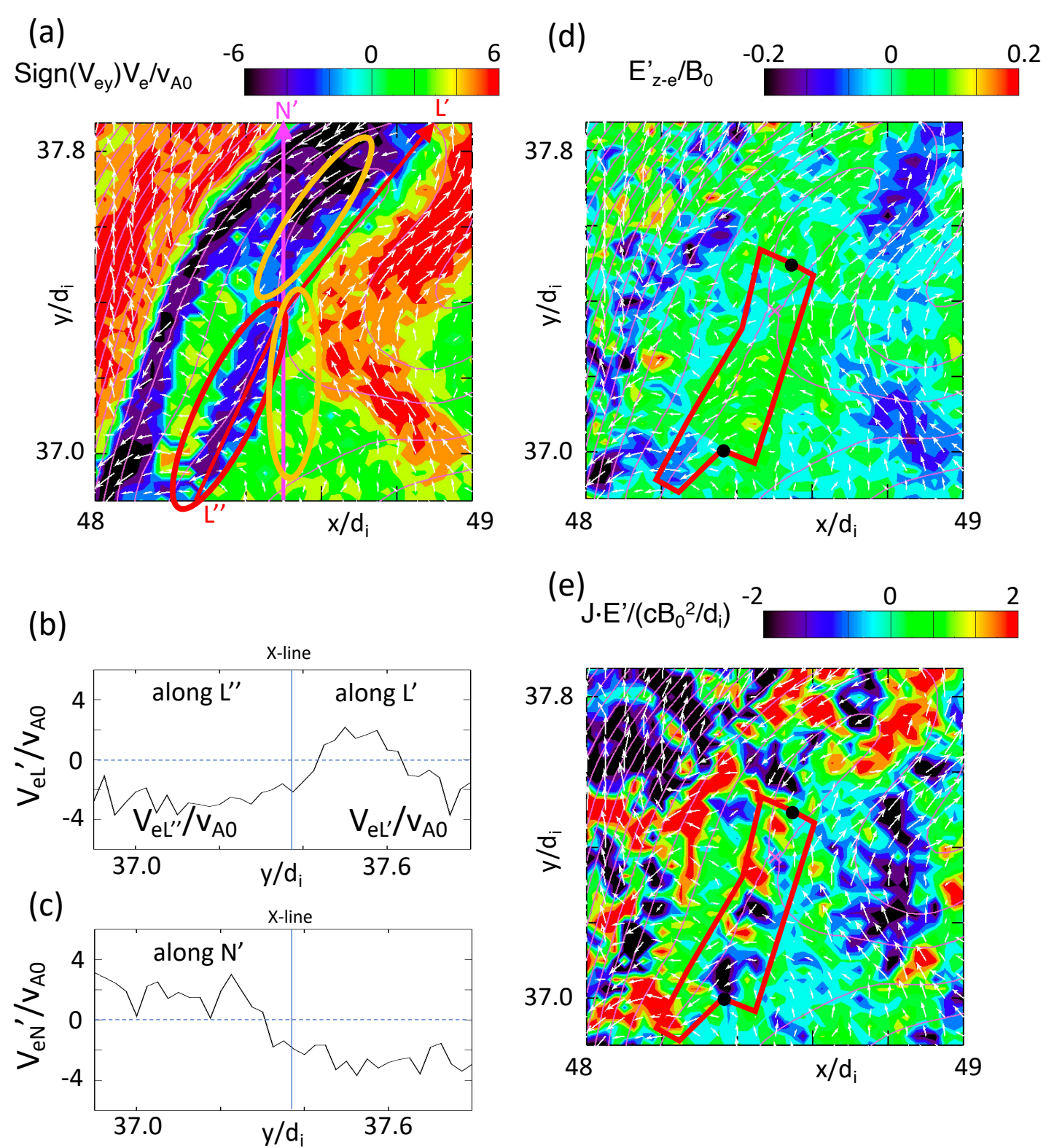


Fig. S2 Electron-only reconnection corresponding to Fig. 3. (a) Electron in-plane velocity  $V_e$  in the X-line rest frame. The orange and red ovals represent the inflow and outflow regions, respectively. The  $L''$  axis is along the outflow, and the  $L'$  axis is along the separatrix in the upper right region. The  $N'$  axis is parallel to the  $y$  axis. The white arrows show the electron fluid velocity vectors. (b) The outflow profile along  $L''$ , and the flow profile along  $L'$ . The blue vertical line is the position of the X-line. (c) The inflow profile along  $N'$ . (d) Contour of the electric field  $E'_{z-e} = E_z + (\mathbf{V}_e \times \mathbf{B})_z/c$ . The region surrounded by red lines represents the EDR. The black dots are the positions of the  $|B_L|$  maxima along the  $N$  axis. (e) Contour of  $\mathbf{J} \cdot \mathbf{E}'$ .

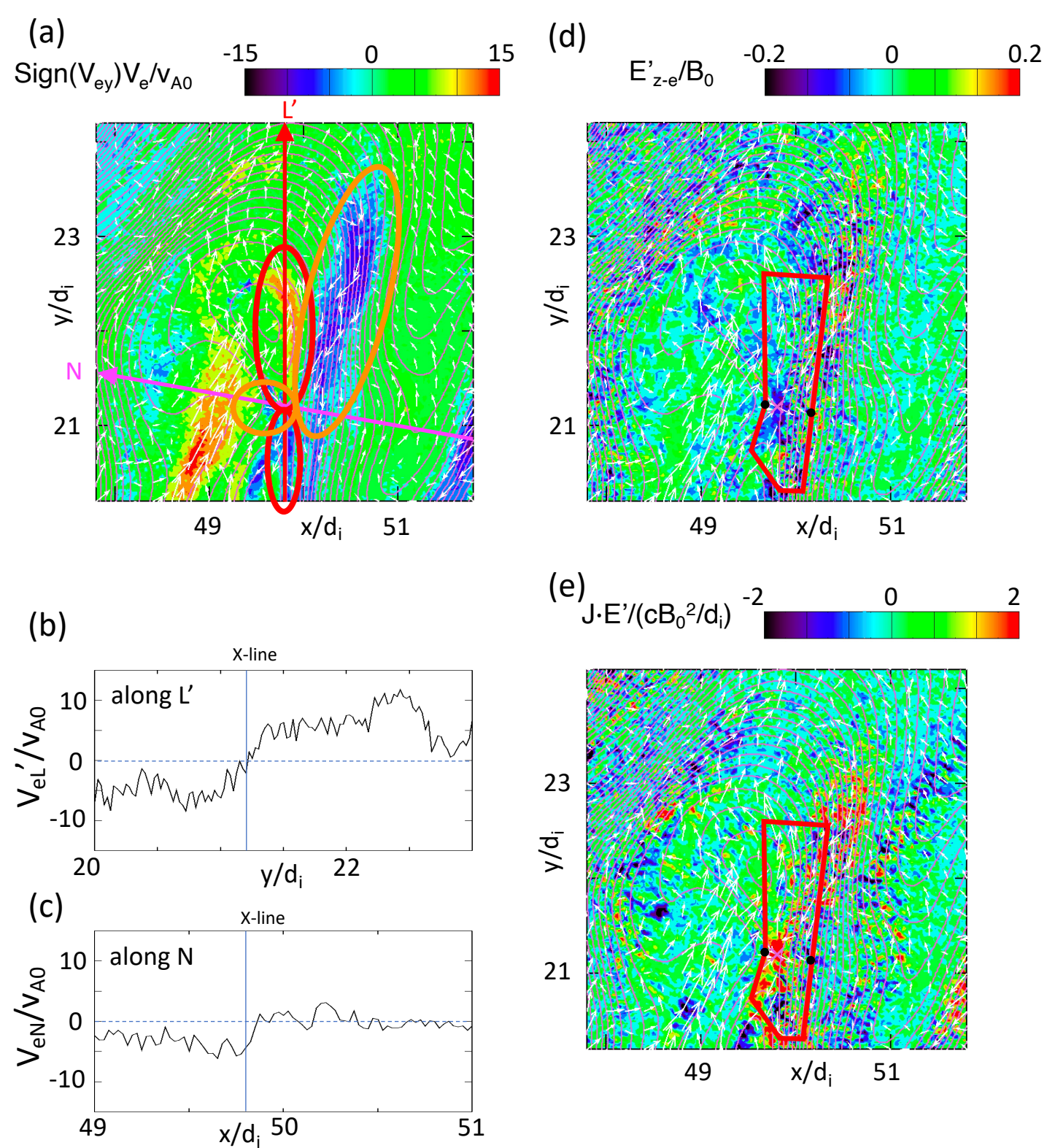


Fig. S3 Regular reconnection corresponding to Fig. 7. (a) Electron in-plane velocity  $V_e$  in the X-line rest frame. The orange and red ovals represent the inflow and outflow regions, respectively. The  $L'$  axis is along the outflow. The  $N$  axis is the same as in Fig.7(d). The white arrows show the electron fluid velocity vectors. (b) The outflow profile along  $L'$ . The blue vertical line is the position of the X-line. (c) The inflow profile along  $N$ . (d) Contour of the electric field  $E'_{z-e} = E_z + (\mathbf{V}_e \times \mathbf{B})_z/c$ . The region surrounded by red lines represents the EDR. The black dots are the positions of the  $|B_L|$  maxima along the  $N$  axis. (e) Contour of  $\mathbf{J} \cdot \mathbf{E}'$ .

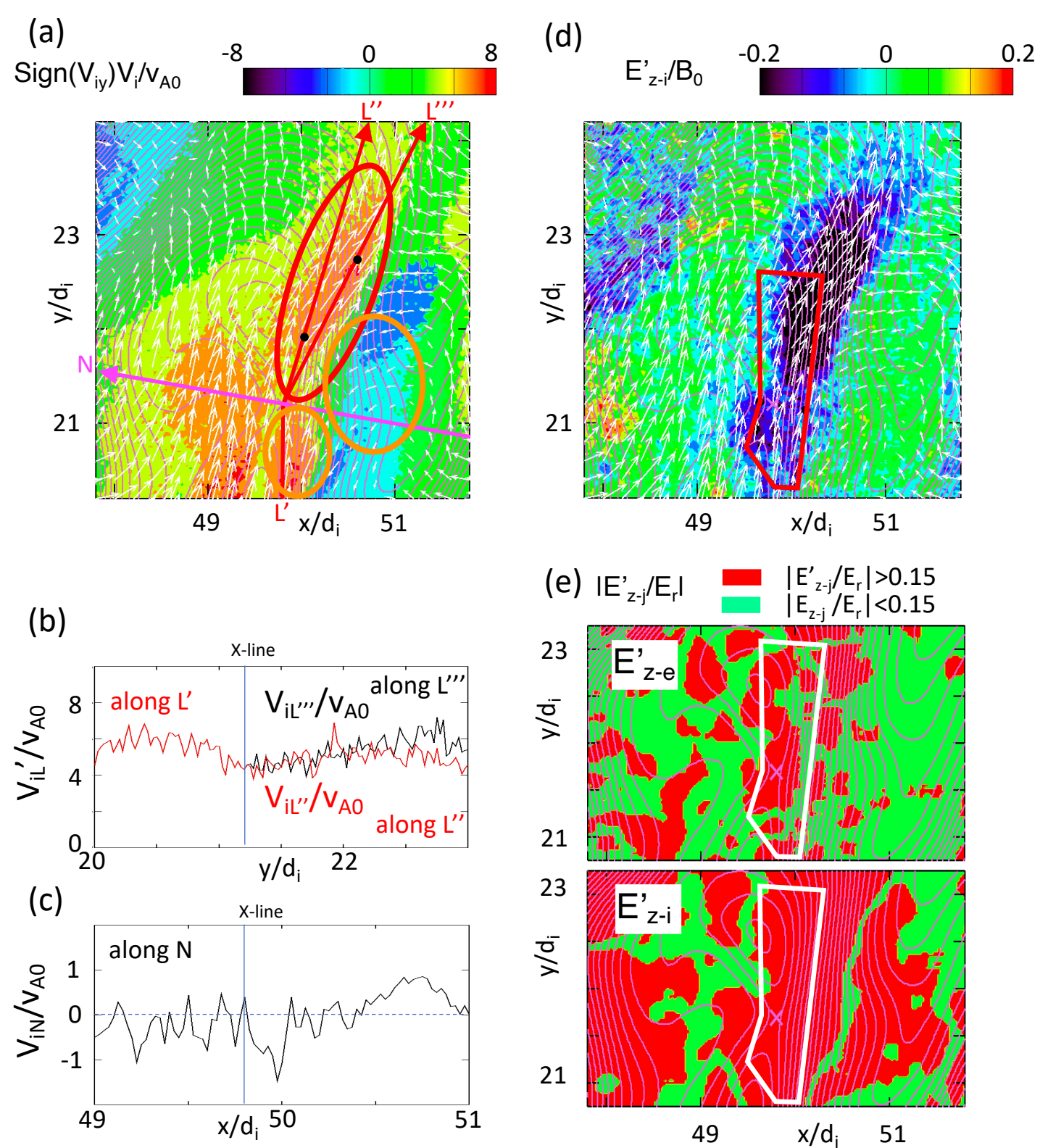


Fig. S4 Regular reconnection corresponding to Fig. 7. (a) Ion in-plane velocity  $V_i$  in the X-line rest frame. The orange and red ovals represent the inflow and outflow regions, respectively. The  $L''$  and  $L'''$  axes are along the outflow, which shows two peaks at the black dots. The  $L'$  axis is along the inflow parallel to the  $y$  axis. The  $N$  axis is the same as in Fig.7(d). The white arrows show the ion fluid velocity vectors. (b) The outflow profile along  $L''$  (red) and along  $L'''$  (black), and the inflow profile along  $L'$ . The blue vertical line is the position of the X-line. (c) The inflow profile along  $N$ . (d) Contour of the electric field  $E'_{z-i} = E_z + (\mathbf{V}_i \times \mathbf{B})_z/c$ . The region surrounded by red lines represents the EDR. (e) (red and green) Contour of  $|E'_{z-e}|$  and  $|E'_{z-i}|$  smoothed using a  $0.25d_i \times 0.25d_i$  window. The normalization  $E_r$  is the reconnection electric field at the X-line.



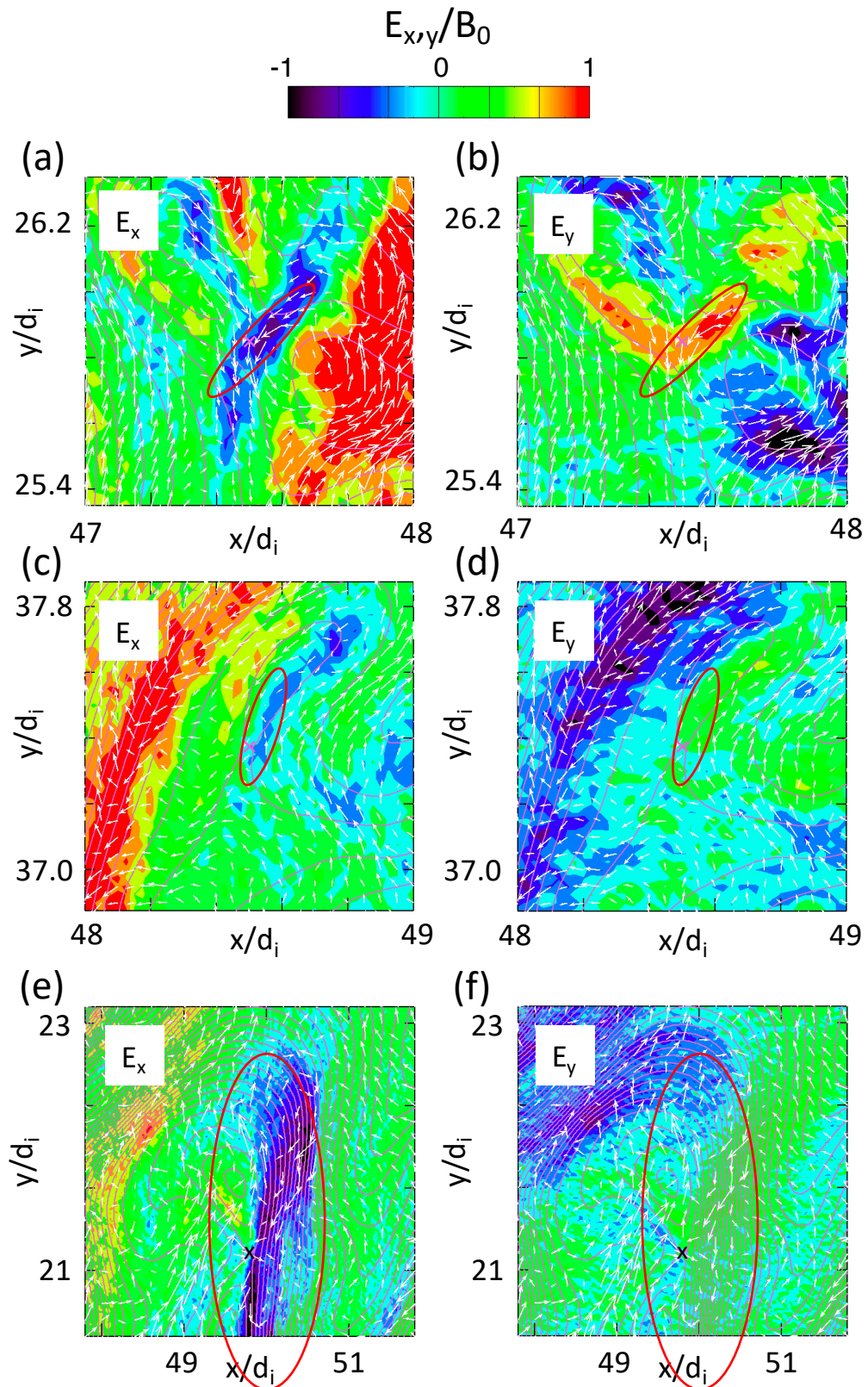


Fig. S5 In-plane electric fields  $E_x$  and  $E_y$  in each reconnection region. Panels (a)(b) are for the electron-only reconnection region corresponding to Fig. 2, panels (c)(d) are for the electron-only reconnection region corresponding to Fig. 3, and panels (e)(f) are for the regular reconnection region corresponding to Fig. 7. White arrows show the electron flow vectors, same as Fig. 2, Fig. 3, and Fig. 7.